*Bulgarian Chemical Communications, Volume 49, Special Edition K2, (pp. 44 – 47) 2017*

# Mechanical properties and microstructure of hot rolled NM360/Q345R composite interface analysis

J. Li[1,3], L. Ma[1,2,3*], G. Zhao[1,2,3], Q. Huang[2,3], X. Yang[1,2,3], M. Cheng[1,2,3]

[1]*Taiyuan University of Science and Technology, Taiyuan 030024,Shanxi,China*
[2]*Shanxi Provincial Key Laboratory of Metallurgical Device Design Theory and Technology,*
[3]*.The Coordinative Innovation Center of Taiyuan Heavy Machinery Equipment*

Received December 13, 2017; Accepted December 20, 2017,

The rolling reduction rate is one of the important factors that affect the bonded reduction rates. The NM360/Q345R composite plates were analyzed by a universal tensile testing machine, OM, SEM and EDS. As the rolling reduction rate increased, both the tensile strength and the elongation increased. When the reduction rates were 30% and 50%, the bonding interface was poor and apparent cracks could be observed after the tensile tests. When the reduction rate reached 70%, no voids or cracks existed, the breaking interface was smooth and neat and the bonding interface formed a common structure. Significant decarbonization of NM360 occurred at the bonding interface. When the reduction rates were 30% and 50%, long strips or black dots of particles appeared near the interface. The black particles were Mn and Si oxides, which could have a negative effect on the bonding interface.

**Key words**: NM360/Q345R, Mechanical properties, Bonded interface, Microstructure.

## INTRODUCTION

The wear-resistant composite steel plate is a new anti-wear composite material manufactured by a cladding technology, which could not only fully utilize the advantage of anti-wear alloys and base materials, but it could also make up for the corresponding shortcomings. Owing to their perfect performance not displayed by other single metals or alloys, the wear-resistant composite steel plates are widely utilized in various industrial fields [1-8].

The wear-resistant composite steel plates are often fabricated by an overlaying technology [9]. During overlaying, the base steel plate is unevenly heated; therefore the gradient of temperature fields is high. This could easily lead to high welding residual stress and deformation. Moreover, the overlaying leads to significant roughness of the overlaying surface, which could cause issues to further machining.

In hot roll bonding [10-12] rolling mills are utilized in the production of composite plates. As a result of the strong force of the rolling mill in combination with the thermal effect, two surfaces of compound metals are pressed together and plastic deformation occurs over the entire metallic cross-section [13].

Until recently, there have been only a few studies on wear-resistant hot rolled bonding plates has been significantly rare. Qiu (2017) studied the effects of rolling and heat-treatment on the structure and properties of the NM450D/ Q235B clad plate [14]. Gong studied the cladding rolling technology of the wear-resistant steel/carbon steel [15].

In this paper, the mechanical properties, the metallographic structure and microstructure of the wear-resistant steel 360 (NM360) - carbon steel Q345R composite plate after vacuum hot rolling were analyzed.

## EXPERIMENTAL PROCEDURE

### *Fabrication of hot-rolled two-layered NM360/Q345R composite*

In this study, the two-layered NM360/Q345R composite was roll-bonded, Q345R, being the base layer and NM360 the cladding layer. The chemical composition of Q345R and NM360 is presented in Table 1.

Firstly, the NM360 and Q345R steels were prepared and underwent surface treatment. The composite surface had to be cleaned and smoothly ground, which allowed the two types of metal atoms to mutually diffuse and reach a metallurgical bonding.

**Table 1**. Main chemical composition of NM360 and Q345R materials (mass fraction %)

| | C | Si | Mn | P | S | Cr | Ni | Mo | B |
|---|---|---|---|---|---|---|---|---|---|
| NM360 | ≤0.25 | ≤0.70 | ≤1.30 | ≤0.025 | ≤0.010 | ≤1.40 | ≤1.00 | ≤0.50 | ≤0.004 |
| Q345R | 0.15 | 0.35 | 1.40 | 0.013 | 0.004 | — | — | — | — |

*To whom all correspondence should be sent:
E-mail: mlf060913@163.com

By a wire brush machine the surfaces were polished until the "sand surface" effect was observed, though the surface roughness surface roughness increase led to the subsequent rolled bonding of the composite.

Subsequently, the polished surfaces were cleaned with absolute ethanol for surface adhesion and oil removal. The surfaces were blown-dried. Secondly, the NM360 and Q345R steels were batched and welded with the clean surfaces facing each other. The composite slab was sealed by argon arc welding and the vacuum evacuating nozzle was welded. Finally, a two-stage diffusion vacuum pump was utilized for the slab to be pumped to the high vacuum state of $1.0\times10^{-3}$Pa and the suction nozzle was sealed at a high temperature by hot pressure.

The NM360 thickness was 3 mm and the Q345R thickness was 10 mm. The NM360/Q345R composite slabs were preheated at 1200°C and held at this temperature for 10 min. Consequently, hot rolling experiments were performed at 0.2 m/s, the stacks were roll bonded with reduction rates of 30%, 50% and 70%, respectively and cooled down in the air, subsequently to rolling. The sizes of the stacks and the rolling conditions of hot rolled composite are presented in Table 2.

### *Microstructure analysis and mechanical tests*

In order to evaluate the rolling reduction effects of the NM360/Q345R composites on the tensile strength, the rolled composites were prepared according to the Chinese Standard GB/T 6396-2008, along the rolling direction. For the tensile fracture type study, the tensile fracture surfaces were observed by a scanning electron microscope (SEM).

The NM360/Q345R composites were polished and etched in a solution of 4% nitric acid and 96% ethyl alcohol. The RD-ND plane microstructure was observed by ultra-deep microscope (OM), scanning electron microscope (SEM) (ZEISS SIGMA FE-SEM) and EDS.

## RESULTS AND DISCUSSION

### *Mechanical properties of NM360/Q345R composite plate*

Fig.1 demonstrates the tensile strength data of the NM360/Q345R composites with various rolling reduction rates. The yield and tensile strength increased along with the elongation, as the rolling reduction rate increased. Regarding the NM360/Q345R composite at 70% rolling reduction rate, the yield and tensile strength reached the maximum of 396.12 MPa and 514.84 MPa respectively, whereas the elongation was the longest, 39.95%. The tensile strength revealed that coherent and well-bonded layers could support each other; this had a direct effect on both the tensile strength and the elongation [16]. The best performance was observed when the reduction rate was 70%.

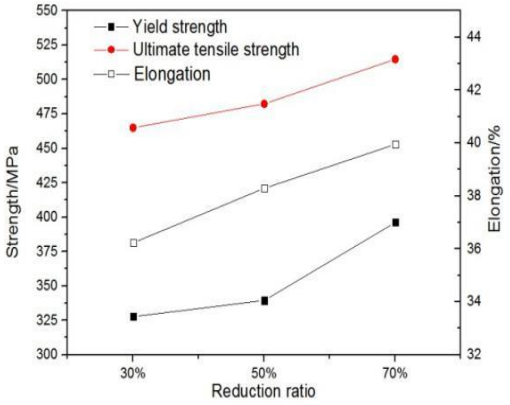


**Fig. 1.** Comparison of mechanical properties of NM360/Q345R composite

### *Tensile fractography*

Fig. 2 a/b presents the fractography at 30% and 50% reduction rate, respectively. Subsequently to tensile failure, an apparent delamination could be observed from the low-magnification picture (100×) in these two conditions, which could be attributed to low bonded strength and poor compatibility of deformation. In NM360 and Q345R a high number of dimples existed, therefore it could be proved that the fracture type of the substrates was ductile. As the reduction rate increased, an increasing number of dimples on the substrates occurred and became increasingly low-sized. It could be observed that the toughness of every single layer was improved as the reduction rate increased, which could also be proved from the tensile mechanical properties.

Fig. 3 presents the tensile fracture morphology at 70% reduction rate. The bonding interface was quite straight and neat, no visible cracks and high-sized pores appeared which proved that the bonding performance was good, as shown in Fig. 3a/b. When the reduction rate increased to 70%, the interface was well-bonded and no delamination could be observed at the interface. Therefore, the bonding strength was high. Through further observation of the fracture morphology (Fig. 3b/c), it could be seen that the substrates near the interface displayed a number of dimples that were the typical ductile fracture feature, demonstrating that a ductile fracture occurred on the substrate. Compared to Q345R or te NM360, the dimples on the interface were quite close and the overall interface was well combined. From the aforementioned discussion, only at a reduction rate of 70%, good bonding between NM360 and Q345R could be obtained under the tested conditions.

**Table 2.** Various base layer thicknesses of rolling compound crafts

| | Plate length+width | NM360 | Q345 | Rolling temperature | Rolling reduction rate |
|---|---|---|---|---|---|
| 1 | 200×100 | 3mm | 9mm | 1150℃ | 30% |
| 2 | 200×100 | 3mm | 9mm | 1150℃ | 50% |
| 3 | 200×100 | 3mm | 9mm | 1150℃ | 70% |

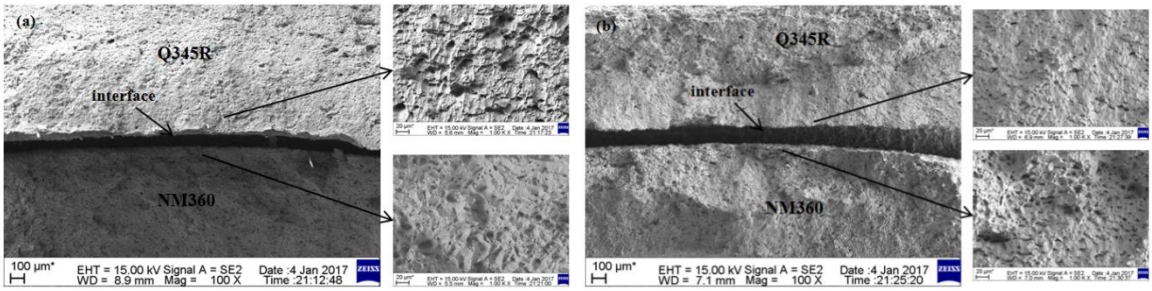


**Figure. 2.** Interface and fracture morphology of NM360/Q345R composite: (a) 30% reduction rate; (b) 50% reduction rate

## CONCLUSION

This paper deduces the coupled flow of the water solution and its components on the basis of the irreversible thermodynamic theory. The results indicate that the effect of clay permeable membrane on the pore fluid flow is not significant. Combining with the potential equilibrium equation controlling the clay crystal swelling potential, the equilibrium equation for forces controlling the clay crystal swelling was developed. Ultimately, based on the modified effective stress laws, considering the physical-chemical coupled flow of the pore fluid in the shale formation and the clay hydration swelling effect, as well as the calculation models for the pore pressure, the effective stresses and the equivalent density of collapse pressure in shale formation were developed. The calculation results indicated that the coupled flow of the drilling fluid in the formation, the clay crystal swelling and the clay osmotic swelling have a significant effect on the borehole stability, and also showed that the effect of the clay crystal swelling is more significant than that of osmotic swelling.

## REFERENCES

1. Y. Zheng， A. Zaoui， I. Shahrour, *Applied Clay Science*, **51**(1), 177 (2011).
2. J. Shi，H. Liu，Z. Lou，Y. Zhang，Y. Meng, Q. Zeng, M. Yang, et al., *Computational Materials Scienc*e, **69**, 95 (2013).
3. F. Salles， J.M. Douillard， O. Bildstein， C. Gaudin，B. Prelot, J. Zajac, H. Van Damme, *Journal of colloid and interface scienc*e, **395**, 269 (2013).
4. T. Schanz， M.I. Khan， Y. Al-Badran, Applied Clay Science, **8**3, 383 (2013).
5. H. Zhao，M. Chen，Y. Li，W. Zhang, *International Journal of Rock Mechanics and Mining Sciences*, **5**4, 43 (2012).
6. X. Chen， C.P. Tan， C. Detournay, *Journal of Petroleum Science and Engineerin*g, **38**(3), 145 (2003).
7. H. Huang，J.J. Azar，A. Hale, Numerical simulation and experimental studies of shale interaction with water-base drilling fluid. 1998.
8. Q. Tao，A. Ghassemi, *Geothermics*, **39**(3), 250 (2010).
9. A. Ghassemi，A. Diek, *Journal of Petroleum Science and Engineering*, 2002. **34**(1): p. 123-135.
10. R. Gelet， B. Loret， N. Khalili, *International Journal of Rock Mechanics and Mining Science*s, **50**, 65 (2012).
11. Q. Wang，Y. Zhou，G. Wang，H. Jiang，Y. Liu, *Petroleum Exploration and Development*, **39**(4), 508 (2012).
12. S. He， W. Wang， M. Tang， B. Hu， W. Xue, Journal of Natural Gas Science and Engineering, **21**, 338 (2014).
13. H. Wen，M. Chen，Y. Jin, K. Wang, Y. Xia, G. Dong, Ch. Niu, *Petroleum Exploration and Development*, **41**(6), 817 (2014).
14. M.E. Zeynali, *Journal of Petroleum Science and Engineering*, **82**, 120 (2012).
15. H. Roshan，M. Fahad, *International Journal of Rock Mechanics and Mining Sciences*, **52**, 82 (2012).
16. E.V. Oort，A.H. Hale，F.K. Mody，S. Roy, *SPE Drilling & Completion*, **11**(03), 137 (1996).
17. R.F.T. Lomba， M.E. Chenevert， M.M. Sharma, Chenevert, M.M. Sharma, *Journal of Petroleum Science and Engineering*, **25**(1–2), 25 (2000).
18. G. Chen，R.T. Ewy，M. Yu, J*ournal of Petroleum Science and Engineering*, **72**(1), 158 (2010).
19. K. Norrish, *Discuss. Faraday Soc*., **18**, 120 (1954).
20. J.C. Parker, *Clays Clay Miner.*, **28**(2), 135 (1980).
21. D. A. Laird, *Clays Clay Miner.*, **44**(4), 553 (1996).
22. N. Alcantar，J. Israelachvili，J. Boles, *Geochimica et Cosmochimica Acta*, **67**(7), 1289 (2003).
23. S.L. Barbour, D.G Fredlund, *Canadian Geotechnical Journa*l, **26**(4), 551 (1989).
24. P.K. Chatterji, N.R. Morgenstern, K.B. Hoddinott，R.O. Lamb, In *Physico-chemical aspects of soils and related materials*, ASTM International, 1095, 118

1990.
25. L. Ge, P. Hu, X.H. Xie, Z. Hu, Q. Zeng, J.B. Liao, *Oxid Commun*, **39**(1), 317 (2016).
26. L. Ge, Z. Hu, P. Chen, L. Shi, Q.Yang, J.B. Liao, *Mathematical Problems in Eng.*, Volume 2014, 1 (2014).
27. L. Ge, Z.Y. Wang, K. Deng, Q. Zeng, X. Wang, X.S. Chen, J.B. Liao, *Journal of the Balkan Tribological Association*, **21**(4), 897 (2015).
28. L. Ge, G.H. Wei, Q. Wang, Z. Hu, J.L.Li, *IEEE Sensors Journa*, **17**(18), 5831 (2017).
29. L. Ge, Q. Zeng, Z.Y. Wang, X.H. Xie, J.B. Liao, J.L. Li, *Oxid Commun*, **39**(1), 240 (2016).
30. R.F.T. Lomba， M.E. Chenevert， M.M. Sharma, *Journal of Petroleum Science and Engineering*, 25(1-2), (2000).